VI International Conference on Particle-based Methods – Fundamentals and Applications
PARTICLES 2019
E. Oñate, M. Bischoff, D.R.J. Owen P. Wriggers, , & T. Zohdi (Eds)

PARTICLE-BASED METHOD FOR INVESTIGATION OF THE PHYSICAL PROCESSES IN THE COMPLEX INDUSTRIAL TASKS

KRAPOSHIN M.[1], EPIKHIN A.[1, 2], MELNIKOVA V.[1, 2] AND STRIJHAK S.[1]

[1]Ivannikov Institute for System Programming of the Russian Academy of Sciences
Solzhenitsyna str. 25, 109004, Moscow, Russia
E-mail: vg-melnikova@yandex.ru, strijhak@yandex.ru web page: http://www.ispras.ru/en

[2]Bauman Moscow State Technical University
Baumanskaya 2-ya str., 5, 105005, Moscow, Russia

Key words: particle, FVM, OpenFOAM, Euler-Lagrange approach, water droplets, injection, jet, wind farm, wind turbines, solvers.

Abstract. The main task of this paper is improved of modeling accuracy and understanding of the physical process which arises in complex industrial tasks using Euler-Lagrange approach. There were two cases under the study. The first one was aimed to study the dynamics of self-organized turbulent structures. A first qualitative insight into the entrainment process in wind farm is obtained through particle tracking. The second case is focusing on developing the Euler-Lagrange approach for the understanding of the physical processes occurring the water droplets injection into a jet. The water droplets, coming out of the special sockets, are simulated by packages (parcels) of particles of a certain mass and size according to the specified flow rate. Parcels moving in the flow, breakup at high speeds, heating and evaporation are investigated.

1 INTRODUCTION

Currently, many of the known basic models (including implemented in commercial foreign packages) use assumptions and methods based on the transfer of single particles or multi-liquid approaches that are convenient for modeling some phenomena but not suitable for describing complex transient processes. Also, the investigations are underway to combine different approaches for expanding the use of models that describe the multiphase flow — for example, models that include the transfer of the interphase boundary and transfer of individual droplets. However natural and experimental estimation, usually, represent significant difficulties and a quite high cost in the case of study of complex physical phenomena. As a result, there is a need for the use of numerical modeling tools and the development of hybrid models of solvers that combine continuum (Euler) and discrete (described in Lagrange variables) systems. This approach provides additional information about the flow pattern and structure and in many cases serves as confirmation or refutation of the hypothesis describing a physical phenomenon.

In this paper, we consider the use of hybrid (Euler-Lagrange) approach for solving two industrial problems. The open source package OpenFOAM has been chosen as the main platform. The first task is devoted to the dynamics of self-organized turbulent structures around wind turbines, where the use of this approach allows conducting research of the phenomenon of ejection. The second is the development and implementation of a hybrid (Euler-Lagrange) approach for modeling the process of interaction water droplets and a high-temperature gas jet.

2 WATER DROPLETS INJECTION INTO A JET

Currently, one of the critical tasks in the rocket and space field is to reduce the acoustic noise from the working engines jets. Various passive and active methods are used to solve this problem at present. One of these methods is the water jets supply in the area of the hot gas propulsion jet. This approach has been the subject of research, which is reflected in a number of papers by various authors [1-5]. A detailed study of gas-dynamic and acoustic processes arising from the use of this technology in real conditions is a significantly complex and expensive task. The heterogeneity of the region in terms of Mach number, multiphase, splashing of water jets, the presence of physical and chemical processes, the possible interaction and reflection of shock waves, etc. - all these features necessitate the use of numerical modeling tools and the development of a hybrid model of the solver capable of correctly reproducing and predicting the phenomena described above.

The solution of such a problem requires an accounting of the droplet propagation in the supersonic flow. To do this, it is necessary to divide the description of the gas-droplet flow into two systems: continuous (Euler) and discrete (Lagrangian).

2.1 Government equations

Taking into account the currently accepted assumptions, the mathematical model consists of three-dimensional Navier-Stokes equations for turbulent super -, trans- and subsonic flows of a compressible gas-droplet mixture, including the mass, momentum and energy conservation equations; turbulent transfer equation, components of the mixture transfer equations, droplets transfer equation, description of the mechanisms of interaction of water and gas flows (evaporation, momentum exchange). The basis for the continuum system was the pimpleCentralFoam solver [6], which is based on a hybrid method of approximation of convective terms and the Kurganov-Tadmor Scheme.

For the Lagrangian (droplet) part as a base was used an OpenFOAM cloud model sprayCloud. This model used a for representation of a gathering of real particles. This construction is plainly made because that it is almost always too computational demanding to simulate all the real particles.

A sphere particle defined by its position x_p, diameter D_p, velocity U_p and density ρ_p. The mass of the particle $m_p = \frac{1}{6}\rho_p \pi D_p^3$. The particle motion is solved by integrating the force balance. The force represents the sum of all relevant forces: drag force from the fluid phase (F_D) and gravity force (F_G).

$$\frac{dx_p}{dt} = U_p \tag{1}$$

$$m_p \frac{dU_p}{dt} = \sum F_i = F_D + F_G = m_p \frac{U - U_p}{\tau_p} + m_p g \tag{2}$$

The relaxation time of the particles (the time it takes for a particle to respond to changes in the local flow velocity):

$$\tau_p = \frac{4}{3} \frac{\rho_p D_p}{\rho * C_D * |U - U_p|} \tag{3}$$

The drag coefficient C_D calculated via function in the dependency of the particle Reynolds number (Re):

$$C_D = \begin{cases} 0.424 * Re, & Re > 1000 \\ 24 * \left(1 + Re^{2/3}/6\right), & Re \leq 1000 \end{cases}$$

Below are the basic equations, special models modifications (injection and phase change models) and its investigation (heat transfer model, breakup model) to create a hybrid Euler-Lagrange approach for simulating the interaction of gas jets with water are proposed.

2.2 Injection Models

In OpenFOAM, there are several diff erent tools for introducing particles in the fluid flow, according to settings specified by the user. These tools are properly called injectors. Several injection models already exist in OpenFOAM, such as cone nozzle, manual injection, patch injection, and others, but water spray socket may have a different shape. Most often, the holes for the flow of water drops represent a slit and there is a hole with a rotating screw at the end of the socket. Two own models of particle injection have been developed: cone nozzle curling injection model and slit injection model.

Cone Nozzle Curling Injection. Model of cone nozzle injection with curling set by next parameters: time start of injection; total mass of parcels for duration of injection; type of initial velocity; injection number of parcels per second; position, radius $\boldsymbol{R_p}$ and direction of the nozzle injection, angle of injection, rotation frequency $\boldsymbol{\omega}$ and direction (clockwise, counterclockwise) and parcels size distribution type.

The full initial parcel injection velocity:

$$\bar{U} = \omega * R_p * \overline{curlDir} + U_{mag} * \overline{dir} \tag{4}$$

$\overline{curlDir}$ – the velocity tangential direction vector; $\overline{dir}$ – the velocity direction vector.

The normal parcel velocity depending from the setting type:

- constantVelocity

$$U_{mag} = constant \tag{5}$$

- flowRateAndDischarge

$$U_{mag} = \frac{\dot{m}}{\rho_p * A} \tag{6}$$

- pressureDrivenVelocity

$$U_{mag} = \sqrt{\frac{p_{inj} - p}{\rho_p}} \tag{7}$$

$\dot{m}$ – mass flow rate of water, kg/s; p_{inj}- injection pressure, Pa.; $A = \pi * R^2$ - area of the outlet, m^2.

On Figure 1 the water particles injection with the next parameters: mass flow rate $\dot{m} = 0.2$ kg/s, injection parcels per second – 10^5, clockwise curling, angle of injection – 30 degrees, outer diameter – 1 mm, omega – 1000 rad/s, particles size from 0.1 to 0.15 mm - in air with pressure p = 101325 Pa and temperature T = 293 K. is shown.

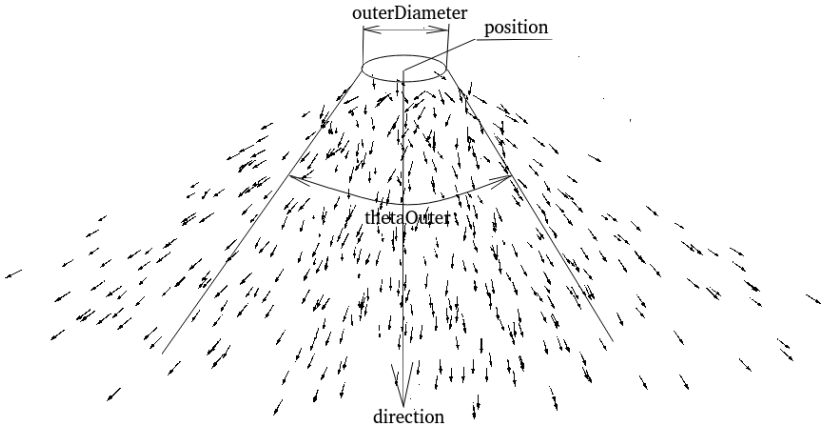

Figure 1: Particles and it's velocity during cone nozzle curling injection

Slit Injection. As the initial parameters for slit injection, besides total mass of parcels, duration, flow type and number parcels per second parameters, using two vectors (*limitDirection 1* and *2*) that determines the spray direction, position of the slit center, slit width (sW) and height (sH).

The full initial parcels velocity calculated by equation:

$$\overline{U} = U_{mag} * \overline{dir} \tag{8}$$

$\overline{dir}$ randomly choose between vectors *limitDirection1* and *limitDirection2*, $A = sW * sH$.

The particle injection with the next parameters: mass flow rate $\dot{m} = 1.0$ kg/s, parcels per second – 10^5, sW = 140 mm, sH = 1 mm, particles size from 0.1 to 0.15 mm – in environment with pressure p = 101325 Pa and temperature 293 K is shown on Figure 2.

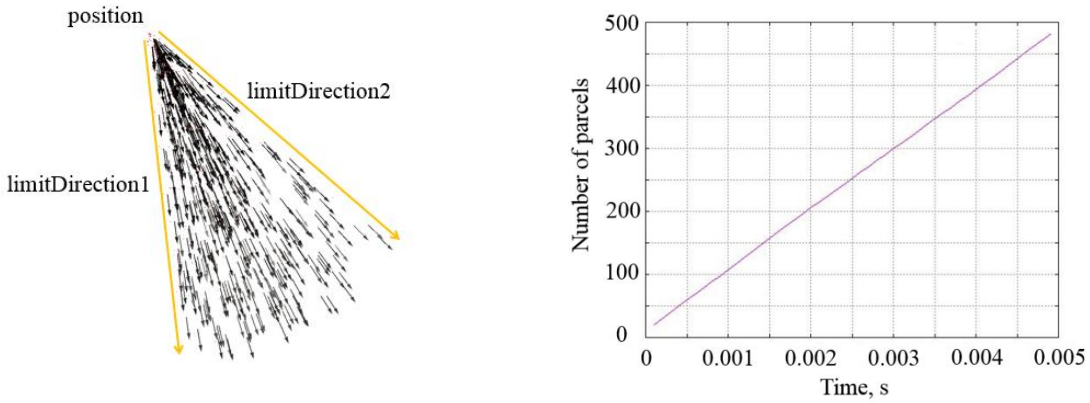

Figure 2: Particles and it's velocity during slit injection.

2.3 Heat Transfer Model

For the calculation of heat transfer from a spherical particle to the surrounding gas, the Ranz Marshall model [7] is used. The Nusselt number can be written:

$$Nu = 2 + 0.6 * \sqrt{Re} * \sqrt[3]{Pr} \quad (9)$$

The test case was made with water parcel with particles 100 μm diameter, mass – $5.2*10^{-9}$ kg and initial temperature 293 K situated in air with the temperature 380 K and 101325 Pa pressure. Gravitational and drag force off. Two variants with motion and steady parcels were considered. The graph on Figure 3 shows that in both cases the system comes to thermodynamic equilibrium, the temperature of the parcels reaches the 373 K and stops. Mass of the parcel, the number of particles and its diameter did not change. When the particles have an initial velocity (U_p=1 m/s), its heating occurs faster.

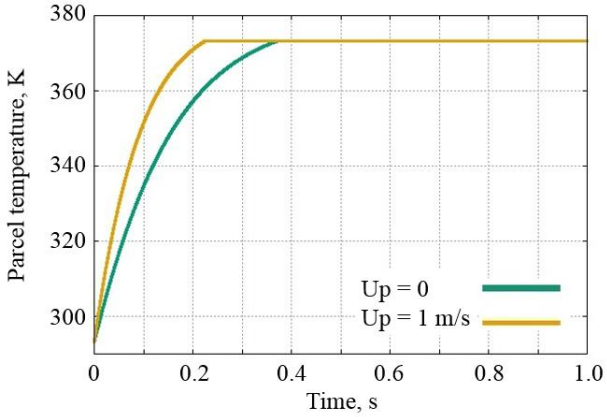

Figure 3: Temperature dependence during time.

2.4 Phase Change Model

The phase change model responds for the evaporation of the droplet. Two models were investigated during simulation. One of them liquidEvaporation model already implemented in OpenFOAM and another one – Spalding model, described in [8], was integrated. Below you can see the verification tests for these models.

Spalding model. The Spalding model realization compared with [8]. According to analytical solution the time of droplet vaporization directly proportional the square of the droplet radius (d^2 law):

$$R_p = \sqrt{R_{p0} - kt} \quad (10)$$

$$k = 2 * \frac{\rho_p}{\rho} * D_{ab} * ln(1 + B_m) \quad (11)$$

R_{p0} – initial particle radius, m; t – time, s; ρ - gas density, kg/m^3; D_{ab} - vapor diffusivity, m^2/s; B_m - Spalding mass transfer coefficient.

The following case was made to confirm it. The unmoved water droplet (diameter - 0.0017 m, mass – $2571*10^{-9}$ kg) evaporates with constant environment temperature 293 K and pressure 101300 Pa. The result is presented at Figure 4.

The changes of the one water droplet temperature in time were compared with simulation and experimental results in [8] (Figure 5). The water droplet with the temperature 301.45 K free fall. The environment temperature is 301.45 K and pressure is 101300 Pa with air relative humidity 0.22. Two variants of saturated pressure calculation were considered: by OpenFOAM

library and by Clausius-Clapeyron equation:

$$pSat = p * Exp[-\frac{H}{R} * (\frac{1}{T_p} - \frac{1}{Tvap})] \quad (12)$$

H - enthalpy of evaporation, 40.7*10^6 Дж/(моль*К)*;* $Tvap$ - temperature of vaporization, 373 K; T_p – particle temperature, K; p – environment pressure, Pa.

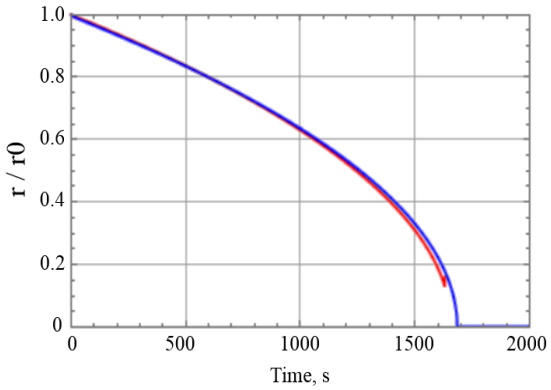

Figure 4: Particle size dependence during time

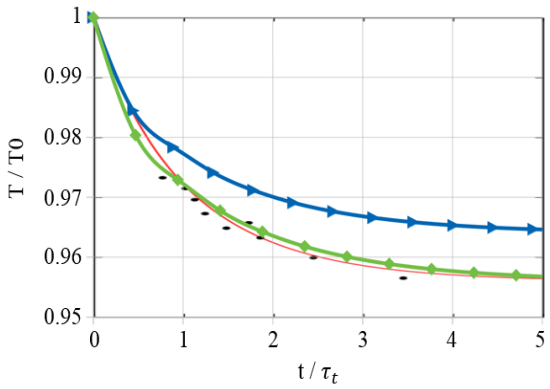

Figure 5: Temperature dependence during time (test 2)
red line – simulation in [2], black dots – experiment [2], green line – simulation (saturated pressure calculated by Clausius-Clapeyron equation), blue line – simulation (saturated pressure calculated in OpenFOAM library)

OpenFOAM liquidEvaporation model. Liquid evaporation model - uses ideal gas assumption. As the test case was chosen the evaporation of the one water parcel with the dimension 100 μm, mass - 5.2*10^{-9} kg and temperature 293 K. The environment temperature – 10000 K and pressure 101325 Pa. Two variants were considered when the particle is unmoved and moving with the velocity 1 m/s. The gravitational and drag forces off.

The graphs on Figure 6 show that the particle heats to the evaporation temperature, particle mass and diameter decrease during time. When the particle have the initial velocity (U_p = 1 m/s), it heating and respectively evaporation occurs faster.

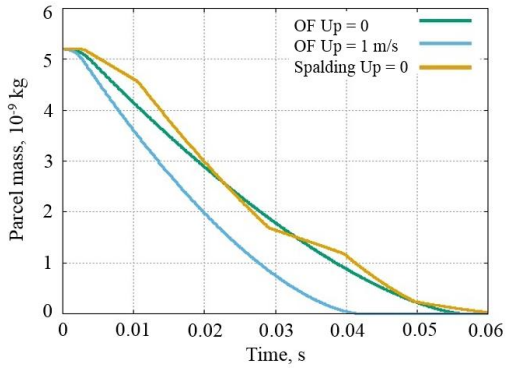

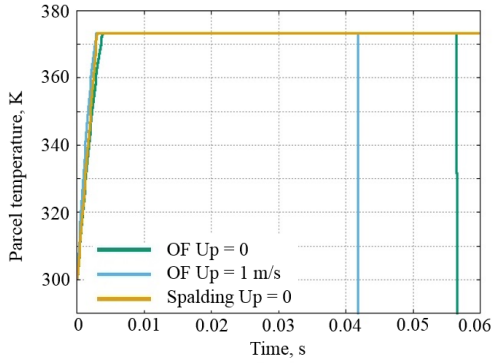

Figure 6: Water mass and maximum particle temperature dependence during time

2.5 Breakup Model

Also, the breakup model was investigated. In our simulations we used a Taylor Analogy Breakup (TAB) Model [9]. This method is based upon Taylor's analogy between an oscillating and distorting droplet and a spring mass system. With the increasing speed of the parcel, the number of droplets should become more, but drops should be a smaller diameter, and respectively evaporates faster. The number by which the drop is divided depends on the Number of Weber.

From the Figure 7 you can see that with the increase of the critical Weber number the mass of the evaporated gas is reduced, a large critical Weber number is similar to disabling a model of the drops breakup.

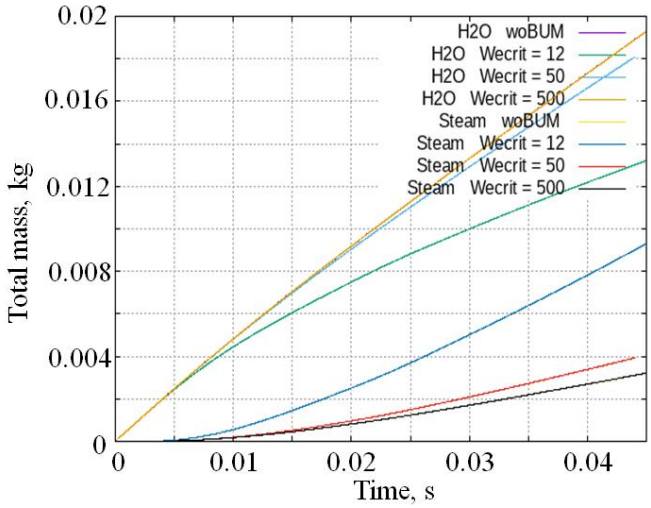

Figure 7: Water and steam phase change in the system with different critical Weber number

3 DYNAMICS OF SELF-ORGANIZED TURBULENT STRUCTURES AROUND WIND TURBINES

Wind energy is an important part of renewable energy sources in many countries. The development of the wind energy industry in Russian Federation (RF) involves the design and operation of new wind power plants and turbines. Wind farms can operate in various climate conditions on the vast territory of RF (Ulyanovsk Oblast, Republic of Adygea, Taman Peninsula, Arctic Region). The first one with 28 wind turbines was constructed in 2017-2018 in Ulyanovsk Oblast. The second one with 3 wind turbines was built in Tiksi in 2018. The new wind farms are building now in Republic of Adygea and in Azov area, and are planned to be built in Krasnodar, Rostov, Stavropol Regions, Republic of Kalmykia till 2022.

The community of researches is normally focused on studying behavior and performance of wind farms, spectral contents of the power fluctuations, different methods of quantifying effects of turbulence-generated loads on wind turbine blade, influence of atmospheric turbulence on the fatigue loads. The turbulent wakes dynamics and wind turbines performance in wind farms

are the questions of the great interest now for the scientific community [10]. Large-eddy simulation (LES) has recently been well applied in the context of numerical simulation of a flow over wind turbines on flat and complex terrains.

The phenomenon of ejection plays a positive role and allows to restore the velocity's deficit in the wake of the wind turbine, therefore, affect the wind capacity of wind farm. The phenomenon of ejection can be studied using the motion of solid particles.

3.1 Computation setup

The open source library SOWFA (Simulator for On/Offshore Wind Farm Application) based on the OpenFOAM is used in this research work. SOWFA includes several incompressible solvers and utilities, being now used actively by the research community, and applies the Large-Eddy Simulation (LES) approach using the finite volume method to solve the governing equations, with different sub-grid-scale (SGS) models relevant for Atmospheric Boundary Layer (ABL) [11]. For instance, the Lagrangian dynamic Smagorinsky model for SGS viscosity can be applied, with an extra constraint on the dynamic Smagorinsky constant C_S used to avoid its negative values which may occur in calculations. The buoyancy effect is inserted by the separate term in the momentum equation in Boussinesq approximation. Effects of topography, environment stratification, Earth rotation, thermal flux changes are all taken into account to compute flow parameters.

The terms in the governing equations, for quantities defined in the mesh cell center, are approximated with the first and second order of accuracy on time and space. The improved iterative PISO algorithm is implemented to solve the system of discretized algebraic equations, using the predictor-corrector procedure and the iterative method of conjugate gradients with a preconditioner for velocity, pressure, potential temperature, stress tensor, and SGS model parameters.

LES with finite volume method for the solution of the main equations reflecting conservation laws was used. The following equations are considered: the continuity equation, the momentum equation, the transport of scalar value - potential temperature equation and other equations for the SGS stress tensor, turbulent viscosity.

The subgrid-scale models are an important part of LES [12]. The SGS stress tensor was raised from the filtering of the Navier-Stokes equations. The Boussinesq approximation for buoyancy force is included with the separate term in the momentum equation.

The Gauss linear Scheme was used for approximation of the convective terms, the Gauss linear corrected scheme was used for approximation of laplacian terms. To solve linear system equations the PBiCG method with DILU preconditioner was used for velocity, temperature and the GAMG method was used for pressure.

The main idea of new solver with the Euler-Lagrange approach, developed in ISPRAS, is based on adding a new KinematicCloud class to the ABLSolver LES solver, which describes a kinematic cloud of particles with equations (1)-(3).

An example of solving an applied wind energy problem for a model wind farms with 12 or 14 wind turbines will be investigated. To determine the initial distribution of parameters, we used the neutral atmospheric boundary layer approximation, calculated using the method Precursor, implemented in the ABLSolver solver. The mathematical modeling of the flow parameters in the wind farm was done using the pisoFoamTurbine solver and the Actuator Line

Model.

3.2 Definition of the problem

The 12 wind turbines in model wind farm were considered in case with SOWFA library. The diameter of rotor for wind turbine was equal to D = 0.416 m. The reference velocity was set to U_{ref} = 1.5 m/s. Atmospheric Boundary Layer model was introduced to represent experimental conditions. The parameters of Neutral ABL, used in our simulation, are listed in Table 1 of work [13].

Each of the prototype wind turbines had 3 blades with constant cross section. The blade was made of carbon fibre with a shape of a twisted thin flat plate of 0.8 mm thickness, without using any aerofoil cross-section [14]. Operating tip-speed ratio (TSR) was set to 6.

The value of numBladePoints for the case with 12 wind turbines was set to 40, the epsilon value was set to 5.0. The data on velocity profile and wind direction were taken from the weather station and the free report in Internet.

The domain with following dimensions was selected: 6.5 m x 5.5 m x 1 m in width (x-), transverse (y-), and height (z-) directions. The resulting unstructured mesh for the test with 12 wind turbines counted 2, 4, 6 millions of cells. After constructing the primary mesh with blockMesh tool the central zone with the turbines array inside was refined twice and an additional refinement was done around each turbine. The final mesh had 6 millions of cells. The pisoTurbineFoam solver was tested on famous Blind-test tutorial with 2 model wind turbines [15] and 12 wind model turbines in climatic tunnel [13, 16].

3.3 Results of simulations

Figure 8 shows distribution of the vorticity field. Propagation of the velocity along the sequence of wind turbines is illustrate in Figure 9. Figure 10 shows normalized mean velocity in different sections of the computation domain.

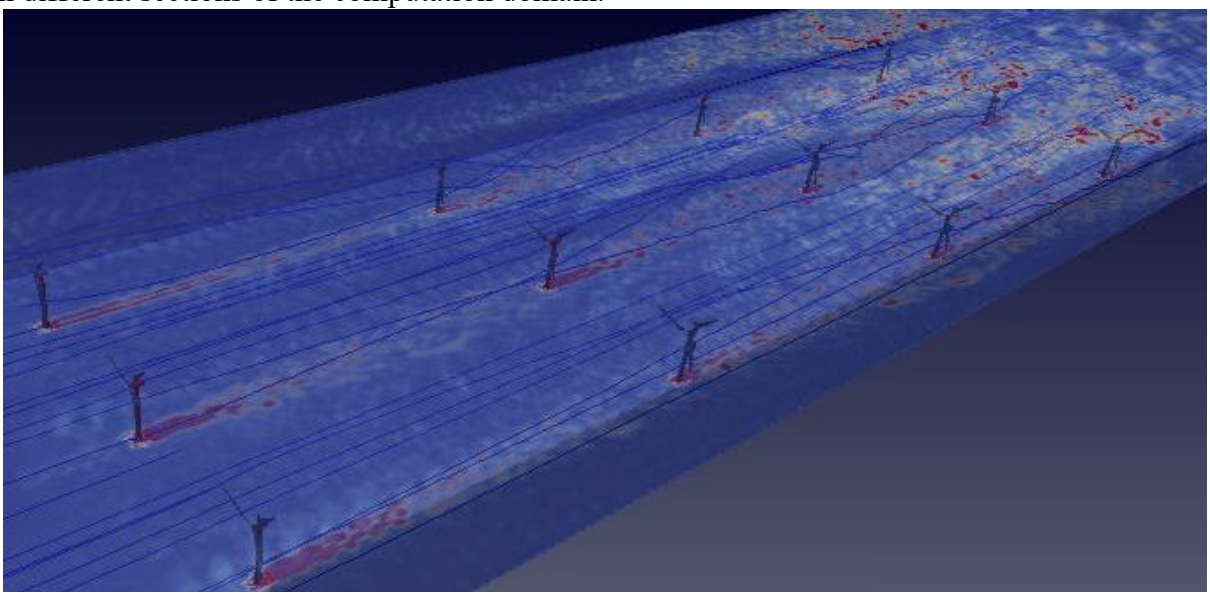

Figure 8: Vorticity field at T_{end} = 20 seconds

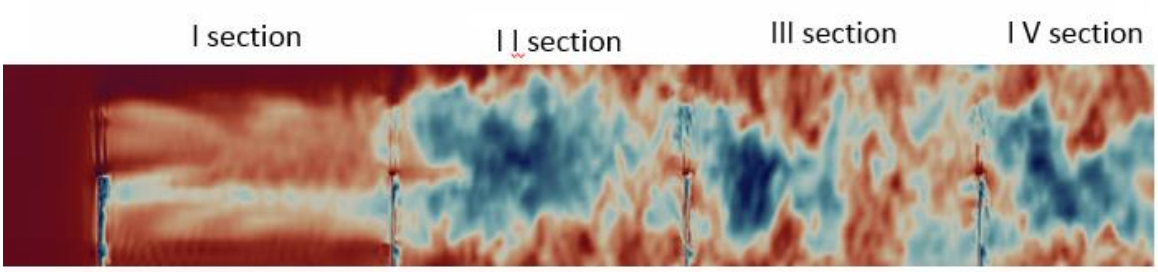

Figure 9: Propagation of the velocity along the sequence of wind turbines

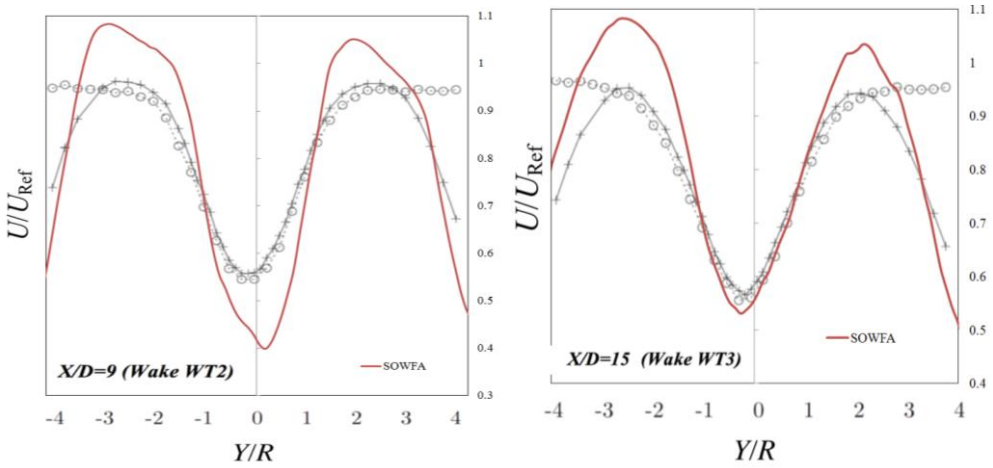

Figure 10: Normalized mean velocity profile

Particles application. The standard injection models in OpenFOAM, such a manual injection, and patch injection were used at the inlet. Solid parcel with the dimension $1*10^{-5}$ m, mass - $1*10^{-8}$ kg and temperature 285 K. The environment temperature – 285 K and pressure 98000 Pa. A first qualitative insight into the entrainment process in wind farm is obtained through particle tracking, where passive particles are released into the flow for every 200th time step. The particles are advected according to the local velocity at each time step. It was defined that there was a high degree of mixing and the initial colour partitioning was broken after turbines 1–2 for both seeding positions. There were also areas, where the particles have essentially been flushed away by the turbulent fluctuations, e.g. between turbines 7–12. The distribution of particles changes significantly over time as they are advected through the wind farm. The distribution of particles from each seeding height is counted within 'imaginary' cylindrical tubes between the turbines.

4 CONCLUSIONS

A study of two developed solvers based on the OpenFOAM package and using the Euler-Lagrange approach was conducted. Validation of the proposed models was carried out with analytical and experimental data. A particle of spherical shape and various models of their injections to the computational domain were considered.

The reported study was funded by RFBR, project number 17-07-01391.

REFERENCES

[1] Tam, C.K.W., Viswanathan, K., Ahuja, K.K., Panda, J. The sources of jet noise: experimental evidence. *Journal of Fluid Mechanics* (2008) **615**: 253-292.

[2] Tam, C.K.W., Golebiowsky, M., Seiner, J.M. On the two components of turbulent mixing noise from supersonic jets. *AIAA-Paper 96-1716* (1996).

[3] Rajput, P., Kumar, S. Jet noise reduction by downstream fluidic injection: effect of injection pressure ratio and number of injection ports. *2018 AIAA Aerospace Sciences Meeting* (2018).

[4] Crighton, D.G. Basic principles of aerodynamic noise generation. *Progress in Aerospace Sciences* (1975) **16, Iss. 1**: 31-96.

[5] Kandula, M., Vu, B. On the scaling laws for jet noise in subsonic and supersonic flow. *NASA Preprint No. KSC-2003-040* (2003).

[6] Kraposhin, M.V., Banholzer, M., Pfitzner, M., Marchevsky, I.K. A hybrid pressure- based solver for nonideal single- phase fluid flows at all speeds. *Int. J. for Num. Meth. In Fluids* (2018) **88, Iss. 2**: 79-99.

[7] Aissa, A., Abdelouahab, M, Noureddine, A., Elganaoui, M., Pateyron, B. Ranz and Marshall correlations limits on heat flow between a sphere and its surrounding gas at high temperature. *Thermal Science* (2015) **19**: 1521-1528.

[8] Barba, F.D., Picano, F. Evaporation of dilute droplets in a turbulent jet: clustering and entrainment effects. *arXiv:1703.0927v1 [physics.flu-dyn]* (2017).

[9] O'Rourke, P. J. and Amsden, A. A. The Tab Method for Numerical Calculation of Spray Droplet Breakup. International Fuels and lubricants meeting and Exposition. United States. 1987.

[10] Andersen, S.J., Sørensen, J.N., Mikkelsen, R.F. Turbulence and entrainment length scales in large wind farms. *Phil. Trans. R. Soc.* (2017) **A 375**: 20160107.

[11] Churchfield, M.J., Lee,S, J. Michalakes, J., Moriarty, P.J. A numerical study of the effects of atmospheric and wake turbulence on wind turbine dynamics. *Journal of Turbulence* (2012) **13, No. 14**: 1–32.

[12] Epikhin, A. S. and Kalugin, V. T. Features of numerical simulation of the unsteady vortex flow around aircraft considering airbrake. *IOP Conference Series: Materials Science and Engineering* (2018) 468(1).

[13] Hancock, P.E. and Farr, T.D. Wind-tunnel simulations of wind-turbine arrays in neutral and non-neutral winds. *Journal of Physiscs: Conference Series* (2014) **524**: 012166.

[14] Hancock, P. E. and Pascheke, F. Wind-Tunnel Simulation of the Wake of a Large Wind Turbine in a Stable Boundary Layer: Part 2, the Wake Flow. *Boundary-Layer Meteorology* (2014) **151**: 23–37.

[15] Kryuchkova, A., Tellez-Alvarez, J., Strijhak, S., Redondo, J. M. Assessment of Turbulent Wake Behind two Wind Turbines Using Multi-Fractal Analysis. *2017 Ivannikov ISPRAS Open Conference (ISPRAS), Moscow, Russia*. (2017): 1-7.

[16] Strijhak, S.V., Koshelev, K.B., Kryuchkova A.S. Studying parameters of turbulent wakes for model wind turbines. *AIP Conference Proceedings.* (2018). **2027. # 030086**: 1-8.